

Determining the spectral types of Aldebaran, Deneb, and Mirach

ALYSSA BULATEK ¹

¹*Department of Astronomy, University of Florida, Gainesville, FL 32611*

ABSTRACT

Identifying known spectral lines in the spectrum of a star allows one to determine the star’s spectral type, which is closely related to the star’s temperature. We observed three stars of varying spectral type (Aldebaran, Deneb, and Mirach) using the Pepito spectrometer at Rosemary Hill Observatory (RHO). We calibrated their spectra using spectra from three arc lamps (mercury, krypton, and neon). We used Deneb as a telluric standard star to correct for the instrumental response of Pepito. We estimate that Deneb is an A type star due to its strong hydrogen Balmer lines ($H\beta$ and $H\gamma$ in particular). Aldebaran and Mirach’s spectra reveal that they are much redder than Deneb, and show possible TiO at various strengths, implying Aldebaran and Mirach are K and M type stars respectively. We present measurements of the equivalent widths of the $H\beta$ and $H\gamma$ lines in Deneb’s spectrum as well as the potential TiO line in Aldebaran and Mirach’s spectra, and compare the equivalent width of Deneb’s $H\gamma$ line to stars in the literature.

Keywords: Aldebaran, Deneb, Mirach, stellar spectral types (2051), stellar spectral lines (1630), A stars (5), K stars (878), M stars (985)

1. INTRODUCTION

Aspects of a star’s spectrum allow us to classify a star into one of several spectral types. These spectral types are related to a variety of physical properties of the star, including its temperature, luminosity, and size. A commonly-used method to classify stars is the Harvard classification system developed by Annie Jump Cannon near the turn of the 20th century (Carroll & Ostlie 2007), which separates stars into the classes O, B, A, F, G, K, and M in order of descending effective temperature. Each of these classes can be subdivided

into sub-classes, denoted by a number (from 0 to 9) immediately after the class letter.

We can estimate the spectral type of a star by using common conceptions about what spectral characteristics are present in which classes of stars. For instance, it is commonly taken that A stars have the strongest hydrogen lines, and that cooler stars like K and M dwarfs have weak hydrogen lines but the strongest metal lines.

In this article, we estimate the spectral types of three stars (Aldebaran, Deneb, and Mirach) using spectra from the Pepito spectrometer at Rosemary Hill Observatory (RHO). In Section 2, we describe how the observations and calibration spectra were taken and how the data were reduced. In Section 3, we describe how the wavelength calibration was performed, how the

stellar spectra were extracted and calibrated, and how equivalent widths of select spectral lines would be estimated. In Section 4, we describe the stellar spectra we derived and present our values for the equivalent widths of the spectral lines we measured. In Section 5, we estimate the spectral type of each star given their spectra, discuss sources of error, and present ideas for further work on the project. We conclude in Section 6.

2. OBSERVATIONS

Observations of Aldebaran, Deneb, and Mirach were taken in 2017 by Sarik Jeram, his lab partner, and their TA. The data were provided to us as bitmap files, so no headers or metadata were available for any of the image files besides what was provided in the filenames (their exposure times). Five spectra of Aldebaran were taken with an exposure time of 3 seconds. Five spectra of Mirach (8 seconds each) were also taken, and only three spectra of Deneb were taken (3 seconds each). Dark frames and flat frames were taken with the appropriate exposure times for the stellar spectra and the calibration lamp images.

2.1. Calibration Lamp Images

In order to wavelength-calibrate these stellar spectra, calibration lamp spectra were taken using mercury, krypton, and neon lamps using exposure times of 0.0625 seconds, 0.6 seconds, and 1 second respectively.

It is important to note that the table that Pepito was resting on was bumped at some point during these observations. To accommodate this, a second set of calibration lamp spectra were taken. However, it is unknown at what point in the data taking process this occurred, so we do not know which stars should be analyzed using which wavelength calibration (pre- or post-bump). Since the files do not have headers, we are unable to ascertain the order of the observations. We performed our wavelength cal-

ibration using the second set of calibration lamp images (presumably post-bump), but this may mean that some or all of our stellar spectra will be wavelength-calibrated incorrectly. If time permitted, we would repeat this analysis with the first set of calibration lamp images.

2.2. Data Reduction

Our data reduction and analysis was written in Python. The Jupyter Notebook used to perform data handling and data analysis is located on my GitHub account.¹ The Jupyter Notebook used for producing our wavelength calibration solution is also on my GitHub account.² In the data reduction process, we first generated composite dark frames for each exposure time as well as a composite flat field image. However, when performing dark subtraction on our final flat field image, something went awry. The dark-subtracted final flat contained a lot of negative values, which should not be the case since flat field images should be illuminated and dark images should not be. Because of this issue, we were unable to produce a normalized final flat image, and so we did not flat-field correct our stellar spectra images.

Additionally, we noticed that the location of Deneb’s spectra vertically on the detector (the non-spectral axis) changed between the first frame and the other frames. We chose to only use this first image of Deneb’s spectrum instead of trying to align the spectra vertically, but aligning and combining the images of Deneb’s spectrum could help to reduce noise in the collapsed spectrum.

3. METHODS

¹ https://github.com/abulatek/classes/blob/main/ast6725/spectroscopy_project/ast6725_spectroscopy_project_bulatek.ipynb

² https://github.com/abulatek/classes/blob/main/ast6725/pepito_wavelength_calibration/ast6725_pepito_wavelength_calibration_bulatek.ipynb

3.1. Wavelength Calibration

The first step in creating final spectra for each of the stars we observed was performing wavelength calibration for the spectrometer. For the latter two calibration lamps, we used the wavelength solution from the previous lamp(s) to inform guesses about the known wavelengths corresponding to pixel positions on the detector. We began this process by collapsing the mercury spectrum, which contained the fewest spectral lines that needed to be identified. We matched the centroids of three peaks in the spectrum to bright lines in the NIST catalog of persistent lines of neutral mercury³ and confirmed that the wavelength solution those lines provided was linear when plotting the known wavelength of the line versus the pixel position of the peak on the detector. We used a third-degree polynomial fit to capture the shape of the wavelength solution more closely than a linear fit, though the function at a glance is well-described by a linear fit. The standard deviation of the residuals for the fit to the mercury wavelength solution were on the order of 10^{-12} Å, indicating a good fit.

We repeated this process for the krypton spectrum. This time, to guess which wavelengths in the NIST catalog of strong lines of neutral krypton⁴ each peak corresponded to, we made an initial guess at their corresponding wavelength using the peak centroid position as an input to the mercury calibration polynomial fit. This helped to identify three lines in the krypton spectrum, which we used to get a krypton wavelength solution with a third-degree polynomial fit. This fit also appeared linear, and had residuals on the order of 10^{-12} Å, indicating a good fit.

³ <https://physics.nist.gov/PhysRefData/Handbook/Tables/mercurytable3.htm>

⁴ <https://physics.nist.gov/PhysRefData/Handbook/Tables/kryptontable2.htm>

Penultimately, we combined the mercury and krypton wavelength solutions to make guesses about which wavelengths corresponded to the peaks in the neon spectrum, which had many more spectral lines. We used the strong lines of neutral neon NIST catalog⁵ to identify five spectral lines in the neon spectrum. We used a fourth-degree polynomial fit to the known wavelengths and peak centroid positions and got a linear wavelength solution for the neon spectrum, with residuals on the order of 10^{-13} Å.

Finally, we combined all of our lines from the mercury, krypton, and neon spectra into one wavelength solution, which is shown in Figure 1. The residuals for a fourth-degree polynomial fit on this solution, which are also shown in Figure 1, were slightly higher than for the individual lamps, but are still small, with a standard deviation of 2 Å. This uncertainty on the wavelength fits that we derive can be used on each wavelength measurement we make going forward.

3.2. Spectral Extraction and Calibration

We extracted a spectrum for each star from our final image for that star by collapsing the 2D spectra vertically. The regions we collapsed were estimated by eye. We then applied our wavelength calibration to these spectra to convert from detector coordinates to wavelength. This yields our “initial spectrum” for each star.

We used Deneb as a telluric standard to remove the instrumental response from our initial spectra. Using a temperature of Deneb of 8525 K, we know what the shape of the spectrum in our wavelength range should be if the spectrum were a perfect blackbody. So, we divided out a fifth-degree polynomial fit to Deneb’s spectrum (masking absorption features) from Aldebaran and Mirach’s spectra (as well as Deneb’s spectrum itself) to remove the instrumental re-

⁵ https://physics.nist.gov/PhysRefData/Handbook/Tables/neontable2_a.htm

sponse, then multiplied each spectrum by the blackbody approximation at the required wavelength range to recover the shape of each stellar spectrum. This yields our “final spectrum” for each star.

3.3. Equivalent Widths

We wrote code to estimate the equivalent widths of spectral lines. This code works by cutting out a portion of the spectrum around a suspected spectral line using a mask defined by the user. Then, a first-degree polynomial is fit to the spectrum in that region to estimate the continuum level and shape. The spectrum is then divided by that polynomial to bring the continuum level to 1, which allows for direct equivalency between the area “under” the spectral line (since these are absorption lines, this area is between the spectral line and the continuum level). After the continuum has been fit and corrected for, a Gaussian fit is performed on the spectrum, including a vertical offset parameter to allow the Gaussian function to rise above a zero baseline. The integral under the Gaussian fit within 3σ of the fit mean of the Gaussian is then calculated, and because of the continuum normalization we performed earlier, the equivalent width is equal to this area.

4. RESULTS

4.1. Stellar Spectra

Our initial spectra for each star, which we derive by applying a wavelength calibration to the collapsed 2D spectral images, are shown in the top parts of Figures 2, 3, and 4 for Aldebaran, Deneb, and Mirach respectively. Aldebaran and Mirach’s spectra look qualitatively similar, with a strong absorption line near 5200 Å already visible. Deneb’s spectrum peaks in the center and has a few strong absorption lines at around 4300 Å and 4850 Å.

After using Deneb as a telluric standard to divide out the instrumental response of the detector from each spectrum and multiplying

Star	Wavelength	Equivalent width (Å)
Aldebaran	5174 ± 2 Å	43 ± 2 Å
Deneb	4317 ± 2 Å	37 ± 2 Å
Deneb	4840 ± 2 Å	29 ± 2 Å
Mirach	5175 ± 2 Å	43 ± 2 Å

Table 1. Equivalent widths estimated for four spectral lines in our dataset. The Deneb lines are close to the wavelengths for $H\gamma$ and $H\beta$ respectively.

each spectrum by a blackbody approximation at Deneb’s temperature, we produced our final spectra for each star, which are shown in the lower parts of Figures 2, 3, and 4 for Aldebaran, Deneb, and Mirach respectively.

4.2. Equivalent Widths

We present estimates of the equivalent widths for four spectral lines in Table 1. There are two spectral lines in Deneb’s spectrum and one each in Aldebaran and Mirach’s spectra which we measured the position and equivalent width of. In Deneb’s spectrum, we suspect that the feature around 4310 Å is the $H\gamma$ line (4340 Å) from the Balmer series and the feature around 4830 Å is the $H\beta$ (4860 Å) line. In Aldebaran’s spectrum as well as Mirach’s, the absorption feature at around 5200 Å is of interest, as it may be a potential metal line, identifying these stars as cooler K or M types.

5. DISCUSSION

We can estimate the spectral type from the stars’ final spectra in Figures 2, 3, and 4. Most obviously, we note that Deneb’s absorption lines at around 4300 Å and 4850 Å are close to the wavelengths of some spectral lines in the Balmer series of hydrogen ($H\beta$ and $H\gamma$ respectively), and their strength indicates that Deneb is an A type star. Aldebaran and Mirach’s peaks are much redder than Deneb’s, so they are likely a lot cooler than Deneb. The absorption feature

near 5200 Å could be a titanium oxide feature, indicating that Aldebaran and Mirach are K and M type stars respectively (judging by their relative strengths, as estimated by eye).

To further help identify their spectral types, we considered the equivalent widths of spectral lines in each stellar spectrum. The Aldebaran and Mirach absorption lines had very similar line profiles, and our fitting process resulted in very similar positions and equivalent widths for these two stars. So, from these results, we have no reason to believe the absorption lines of one star is deeper than the other, and thus it would not be unreasonable to say these stars might have a similar stellar type. Due to lack of time, the author was unable to find literature values to compare equivalent widths to for cooler stars.

Deneb’s line widths (37 ± 2 Å and 29 ± 2 Å for “H γ ” and “H β ” respectively) are easier to directly compare to the literature, though the author was unable to find a reference for equivalent widths of H β in stars. If we assume these are lines in the Balmer series, we can compare our H γ equivalent width to values from Cananzi et al. (1993) for other A type stars. H γ equivalent widths for A type stars are highest for A5 stars, but only reach around 16 Å. There may be additional broadening from a physical process within Deneb or along the path from Deneb to the Earth to cause the broader line width we observe. It is also possible that our wavelength calibration, if incorrect, is causing an increased line width. Nevertheless, these Balmer lines allow us to estimate that Deneb might be an A type star.

We can make some qualitative assessments of the wavelength calibration from line identification estimates. In Deneb’s spectrum, our measurements of the two Balmer series lines stray from the literature values by about 20 Å. This is well above our measurement uncertainty of 2 Å, so this indicates that our wavelength solution may be poor. If time permitted, a re-analysis of each stellar spectrum using the other set of calibration lamp images may produce more accurate line centroids and result in equivalent widths closer to the literature values.

6. CONCLUSIONS

We have presented optical spectra of three stars taken in 2017 which were used to estimate the stars’ spectral classes. The spectra were wavelength-calibrated using data from three calibration lamps. The stellar spectra were then corrected for instrumental response using one of the stars, Deneb, as a telluric standard. These spectra were assessed qualitatively to estimate their stellar types, and it is estimated that Deneb is an A type star from its strong presumable hydrogen Balmer lines and blueward peak. Aldebaran and Mirach, on the other hand, are more likely to be cooler K or M dwarfs, which have redward peaks and possible metal lines. A method for measuring equivalent widths was presented, and estimates for the equivalent widths of a spectral line in each stellar spectrum (two for Deneb) were given.

ACKNOWLEDGMENTS

The author wishes to thank Sarik Jeram for acquiring the data for this project and for providing useful feedback along the way.

REFERENCES

- Cananzi, K., Augarde, R., & Lequeux, J. 1993, A&AS, 101, 599
- Carroll, B., & Ostlie, D. 2007, An Introduction to Modern Astrophysics (Pearson Addison-Wesley). <https://books.google.com/books?id=M8wPAQAAMAAJ>

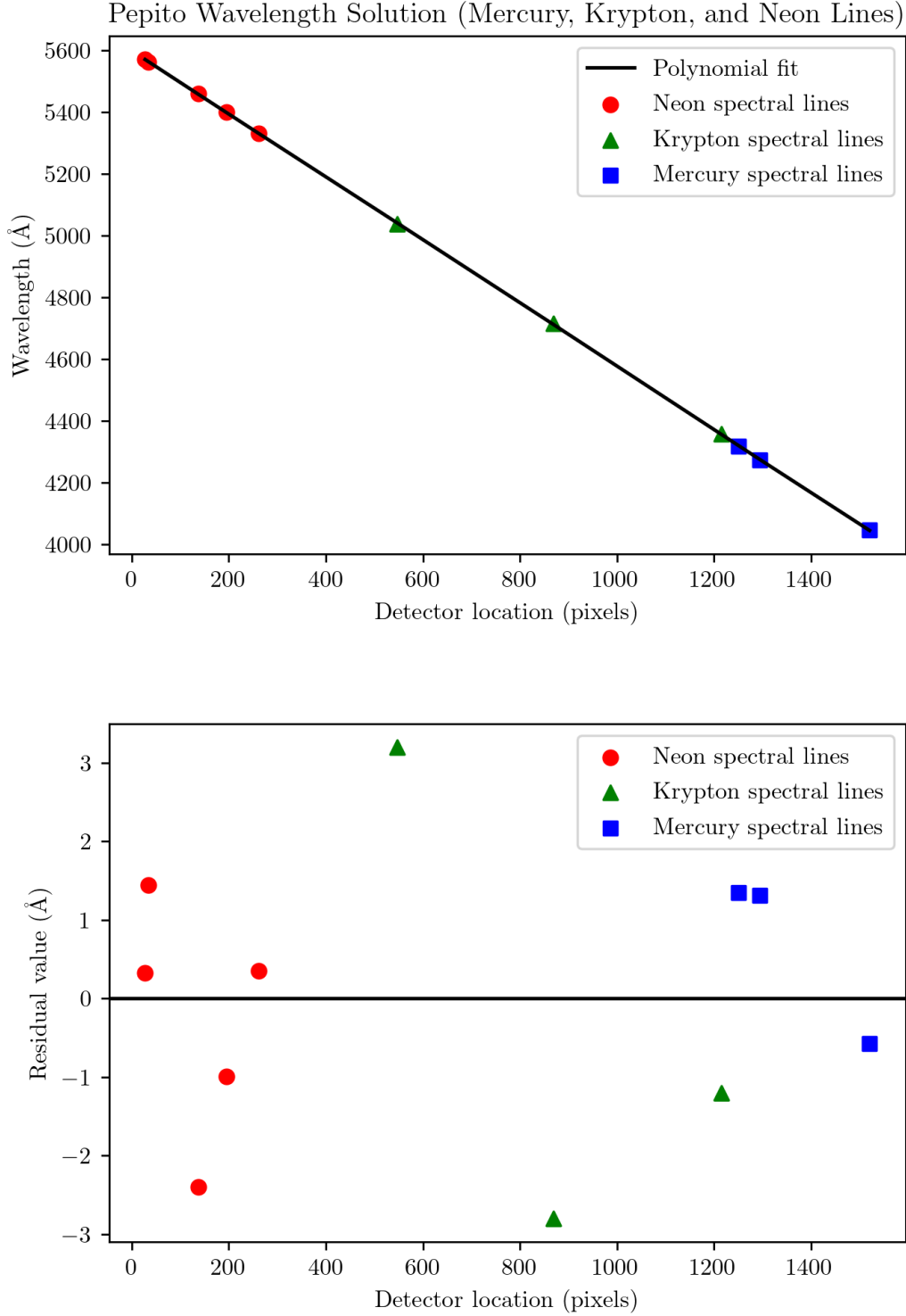


Figure 1. *Above:* Derived wavelength solution for Pepito using spectral lines from the neon (red circles), krypton (green triangles), and mercury (blue squares) calibration lamps. The fourth-degree polynomial fit to these points is shown as the solid black line; the fit is linear to the eye. *Below:* residuals to the fourth-degree polynomial fit to the wavelength solution. The standard deviation of the residuals about their mean (10^{-13} , the horizontal black line) is 2 Å.

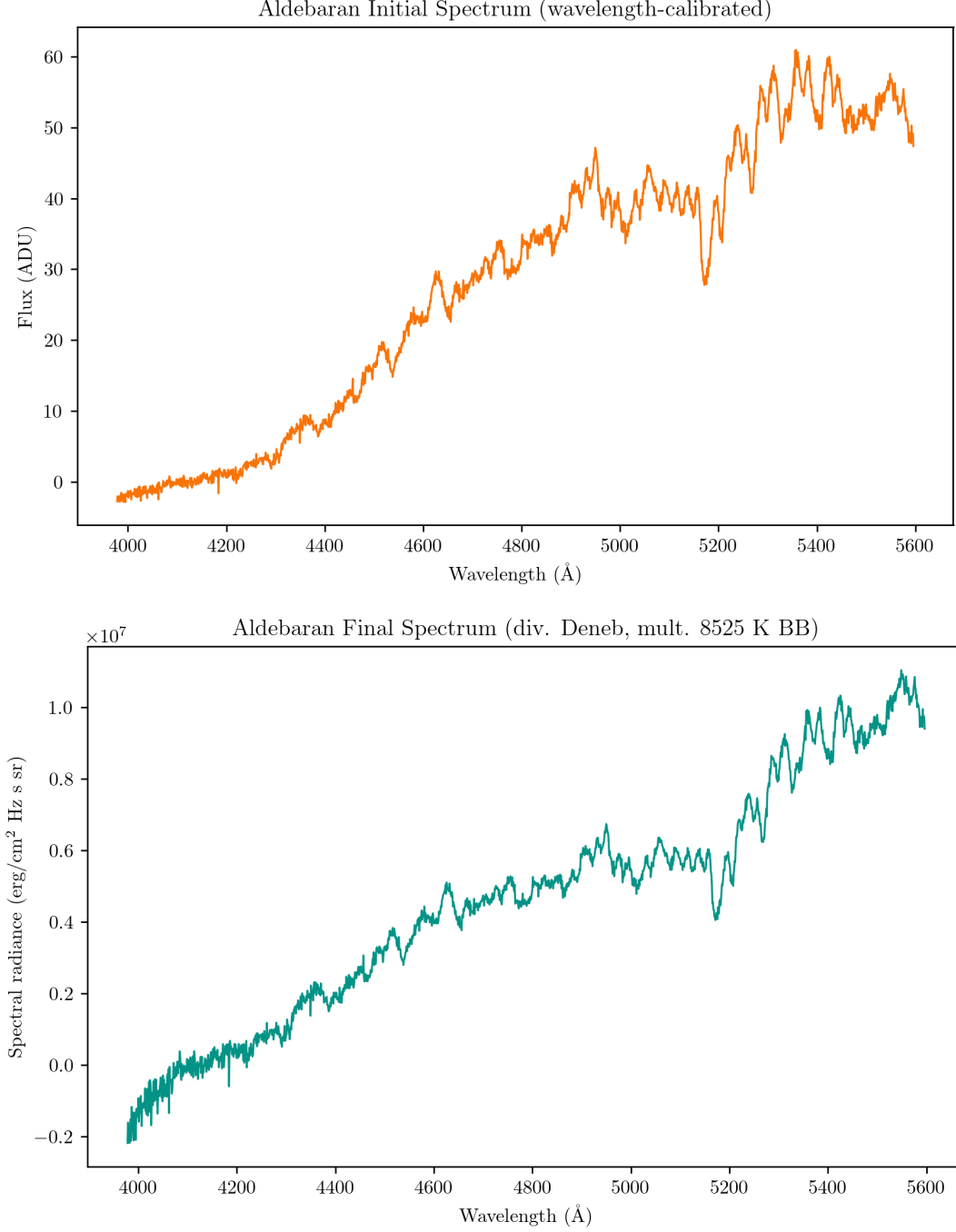


Figure 2. *Above:* initial spectrum for Aldebaran in instrumental units, derived by applying a wavelength solution to the collapsed 2D spectrum. Initially, we see that Aldebaran peaks towards redder wavelengths. There is a strong absorption feature near 5200 Å. *Below:* final spectrum for Aldebaran in units of spectral radiance, which was derived by dividing the spectrum by a polynomial fit to Deneb’s spectrum (to avoid transferring noise or spectral lines) and then multiplying by the blackbody approximation at Deneb’s temperature. This largely resembles the initial Aldebaran spectrum.

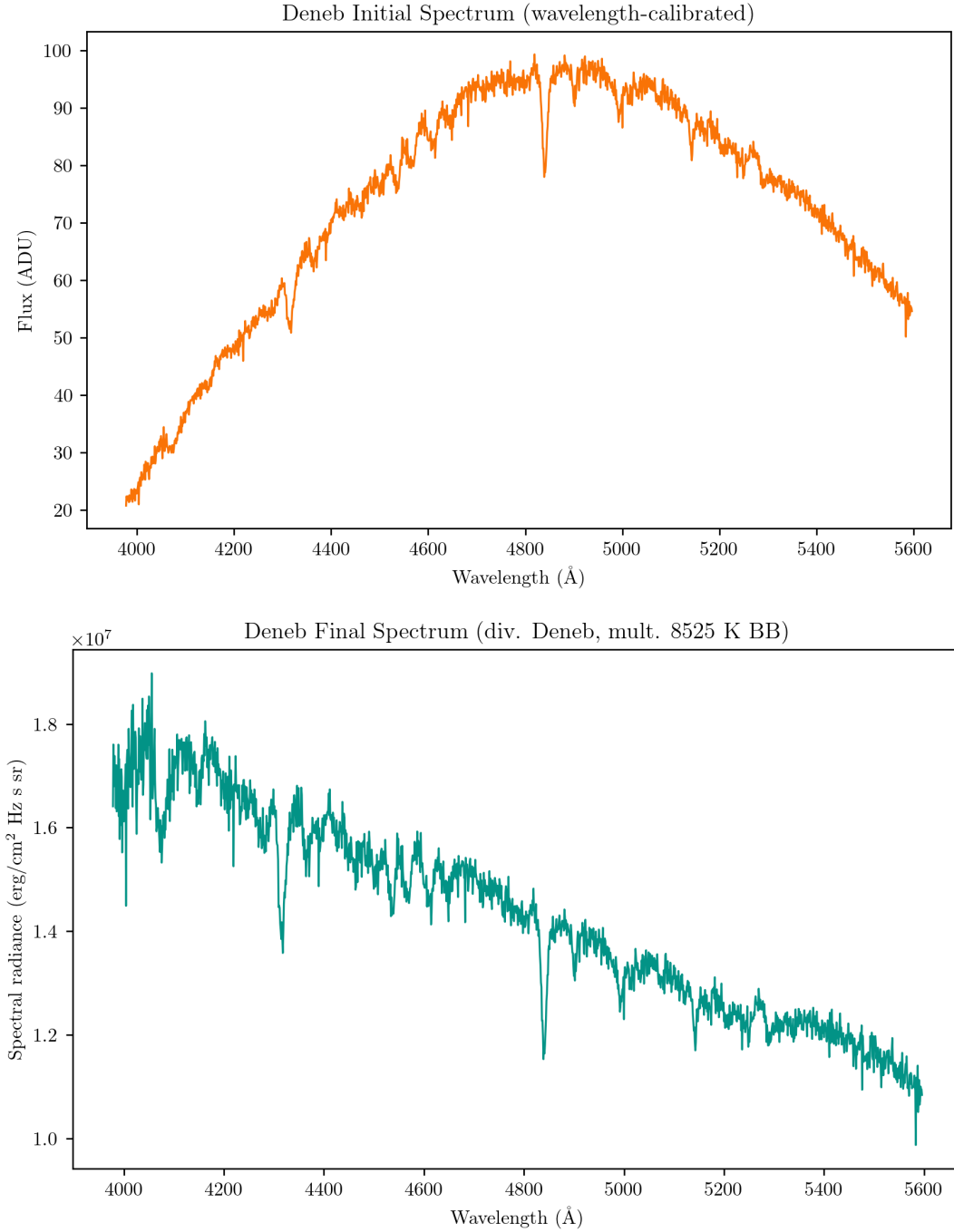


Figure 3. *Above:* initial spectrum for Deneb in instrumental units, derived by applying a wavelength solution to the collapsed 2D spectrum. From this spectrum, we know that Deneb is hotter than Aldebaran and Mirach because its peak is more blueward. We can see strong absorption features near 4300 Å and 4850 Å. *Below:* final spectrum for Deneb in units of spectral radiance, which was derived by dividing the spectrum by a polynomial fit to Deneb’s spectrum (to avoid transferring noise or spectral lines) and then multiplying by the blackbody approximation at Deneb’s temperature. This greatly changes Deneb’s spectrum, showing its peak even more blueward than its initial spectrum.

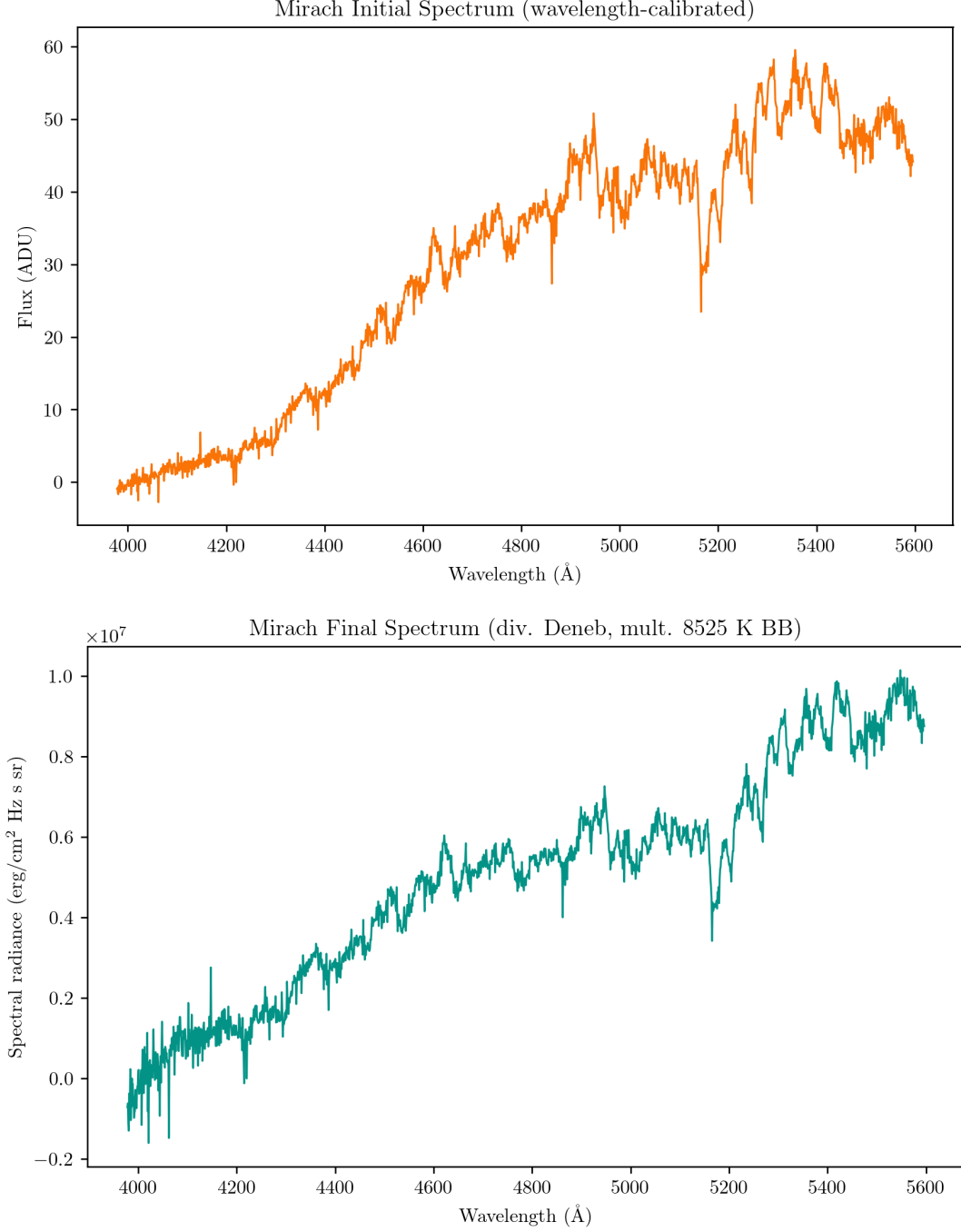


Figure 4. *Above:* initial spectrum for Mirach in instrumental units, derived by applying a wavelength solution to the collapsed 2D spectrum. Initially, we see that Mirach peaks towards redder wavelengths. There is a strong absorption feature just below 5200 Å. *Below:* final spectrum for Mirach in units of spectral radiance, which was derived by dividing the spectrum by a polynomial fit to Deneb’s spectrum (to avoid transferring noise or spectral lines) and then multiplying by the blackbody approximation at Deneb’s temperature. This largely resembles Mirach’s initial spectrum.